

# Design and control of dual servo actuator for near field optical recording system

Jaehwa Jeong<sup>\*a</sup>, Young-Man Choi<sup>a</sup>, Jun-Hee Lee<sup>b</sup>, Hyoung-Kil Yoon<sup>c</sup>, Dae-Gab Gweon<sup>a</sup>

<sup>a</sup>Nano Opto-Mechatronics Lab., Dept. of Mechanical Engineering, KAIST, 373-1 Gusong-Dong, Yuseong-Gu, Daejeon 305-701, South Korea

<sup>b</sup>Dept. of Advanced Industrial Technology, Korea Institute of Machinery & Material, 171 Jang-dong, Yuseong-Gu, Daejeon 305-343, South Korea

<sup>c</sup>Devices and Materials Lab., LG Electronics Institute of Technology, 16 Woomyeon-Dong, Seocho-Gu, Seoul 137-724, South Korea

## ABSTRACT

Near field recording (NFR) has been introduced as a new optical data storage method to realize higher data density beyond the diffraction limit. As the data density increases, the track pitch is remarkably reduced to about 400nm. Thus, more precise actuator is required and we propose a dual servo actuator to improve the accuracy of actuator.

The proposed dual servo actuator consists of a coarse actuator and a fine actuator, multisegmented magnet array (MSMA) voice coil motor (VCM) and PMN-PT actuator. In design of VCM actuator, a novel magnetic circuit of VCM with MSMA is proposed. It can generate higher air gap flux density than the magnetic circuit of VCM with the conventional magnet array. In design of fine actuator, the fine actuator including PMN-PT single crystal instead of the conventional PZT is proposed. The displacement gain of PMN-PT fine actuator is 26 nm/V and that of PZT fine actuator is 17 nm/V. The displacement gain is increased by 53 %.

To evaluate tracking performance of the manufactured dual servo actuator and to assign the proper role to each actuator, the PQ method is selected. From experiment results, the total bandwidth of the dual servo actuator is increased to 2.5kHz and the resolution is 25 nm. Comparing with the resolution of one servo actuator, 70 nm, we can find that the accuracy of actuator is remarkably improved. And the proposed dual servo actuator shows satisfactory performances to be applied to NFR and it can be applied to other future disk drives.

**Keywords:** Voice coil motor, PMN-PT, near field recording, dual servo control

## 1. Introduction

The improvement of multimedia technology has been increasing the data capacity managed by each person continuously. Naturally, the data areal density of disk drive device should be increased. However, there are limits to increase data storage density in the conventional devices. Near field recording (NFR) is proposed as a candidate for the next generation optical data storage device and it is pursuing high data storage density.[1][2] In the conventional optical data storage devices such as CDs and DVDs, they are based on focusing propagating light with an objective lens. As the spot size cannot be less than the wavelength of the light due to the diffraction limit, the maximum density of the conventional optical data storage device is limited. NFR has been introduced to realize higher density recording beyond the diffraction limit.

As the data density increases, the track pitch is reduced to about 400nm. Compared with 1.6 $\mu$ m-track pitch of CD and 740nm-track pitch of DVD, we recognize that track pitch is remarkably reduced and the more precise actuator is required. In this paper, dual servo actuator for application to NFR is proposed and manufactured to improve the accuracy of actuator.

---

\* [capijh@kaist.ac.kr](mailto:capijh@kaist.ac.kr); phone +82-42-869 8763; fax +82-42-869-8763; nom.kaist.ac.kr

## 2. Dual servo actuator design

### 2.1. Structure

Figure 1 shows the total structure of NFR system. NFR system uses solid immersion lens (SIL) which is made of a high refractive index ( $>1.0$ ) to make the numerical aperture (NA) high. Within the near-field range below the SIL, the spot size is less than the wavelength of the light. It is an important fact that the gap between the bottom of SIL and recording surface should be maintained less than 100nm. To satisfy this condition, the air-bearing slider technology is adopted.[3][4] Thus, the focusing actuator used in the conventional optical disk drives is not necessary in the new optical recording system. Fine actuator moves suspension and slider containing SIL and the fine actuator assembly is attached to underneath of coarse moving part as shown in figure 2.

In this system, rotary type voice coil motor (VCM) is selected as a coarse actuator. Generally, the rotary type VCM has faster seeking characteristic than linear type VCM because of its lever structure. In design of VCM actuator, a novel magnetic circuit of VCM with multi-segmented magnet array (MSMA) is proposed. It can generate higher air gap flux density than the magnetic circuit of VCM with the conventional magnet array.[5] High flux density in the air gap generates large actuating force and it makes the seek time short although relatively heavy optical components are loaded on the coarse actuator. The comparative analysis results between the conventional magnet array and MSMA show 13.6% increase in the normal component of the flux density without any change of total thickness, air gap thickness, and magnet area.

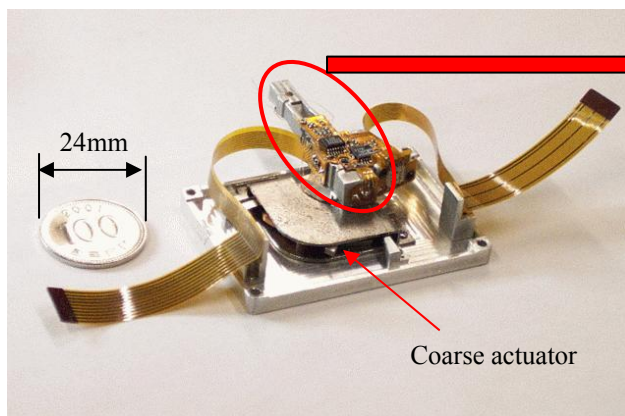


Figure 1: Structure of NFR dual servo actuator

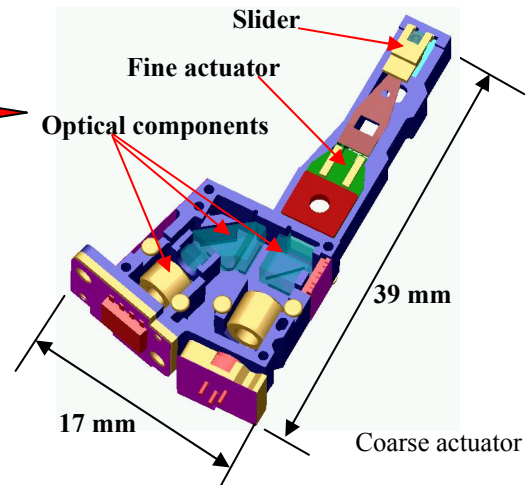
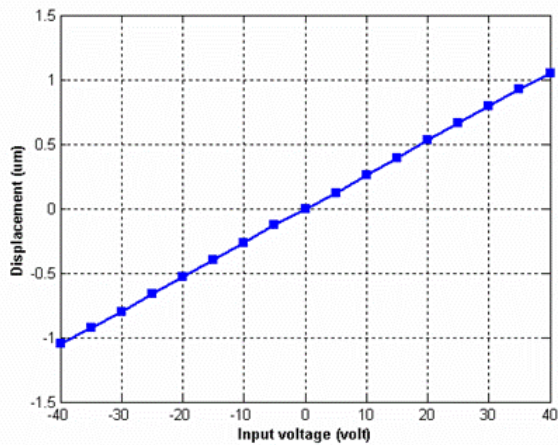
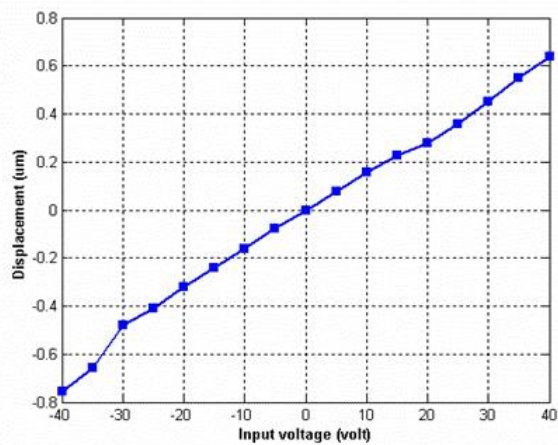


Figure 2: Detail structure of coarse moving part



(a) PMN-PT



(b) PZT

Figure 3: Displacement test results of fine actuators

As the data recording density is higher, the demand for a higher bandwidth servo system which can position the read/write head quickly and precisely on an extremely narrow track width becomes more pressing. To increase the servo bandwidth and to provide fast and accurate positioning of the head, a fine actuator using piezoelectric material is proposed.[6] One of the major drawbacks of piezoelectric fine actuator is high driving voltage. It's an obstacle to commercialize since voltage on current disk drives is limited. The demand for the fine actuator that requires low driving voltage per moving range is increasing. Therefore, the fine actuator including PMN-PT single crystal instead of PZT is developed in this paper. The  $d_{31}$  value of PMN-PT is larger than that of PZT. The displacement gain test results of PMN-PT fine actuator and PZT fine actuator are shown in figure 3 (a) and (b). The displacement gain of PMN-PT fine actuator is about 26 (nm/V) and that of PZT fine actuator is about 17 (nm/V). It is increased by 53 %.

## 2.2. Actuator modeling

System identification technique based on experimental results is applied to get the models of coarse and fine actuators. The experiments are carried out by using frequency sweeping method and the frequency response function of actuator is obtained. Dynamic signal analyzer, HP 35670A, generates sinusoidal signal from 100 Hz to 20 kHz. The signal is applied into the coil in coarse actuator through VCM amplifier and output displacement is measured by laser doppler vibrometer (LDV).

Figure 4 (a) represents the measured frequency response of coarse actuator and its identified model. Based on the transfer function between input current and measured displacement, the transfer function of the coarse actuator is identified by using least square estimation method. The transfer function is expressed by the following equation taking into account the mechanical resonance and the characteristics of the amplifier. Coarse actuator has a mechanical resonance of 4.9 kHz. The identified transfer function of coarse actuator is represented in equation (1).

$$P_{coarse}(s) = -2.235 \times 10^7 \frac{(s + 6932)(s - 2.533 \times 10^4)}{s^2(s^2 + 1446s + 9.511 \times 10^8)} \quad (1)$$

The fine actuator dynamics are measured by the same method which is used in the coarse actuator dynamics experiment. Fine actuator is modeled as a second order system taking into account the mechanical resonance. Dynamic property of the driver has flat gain and no phase lag until 30 kHz. Thus, it can be regarded as a simple gain factor. The identified result is shown in figure 4 (b) and the identified model of fine actuator is described in equation (2).

$$P_{fine}(s) = \frac{1.545 \times 10^8}{s^2 + 1855s + 1.377 \times 10^9} \quad (2)$$

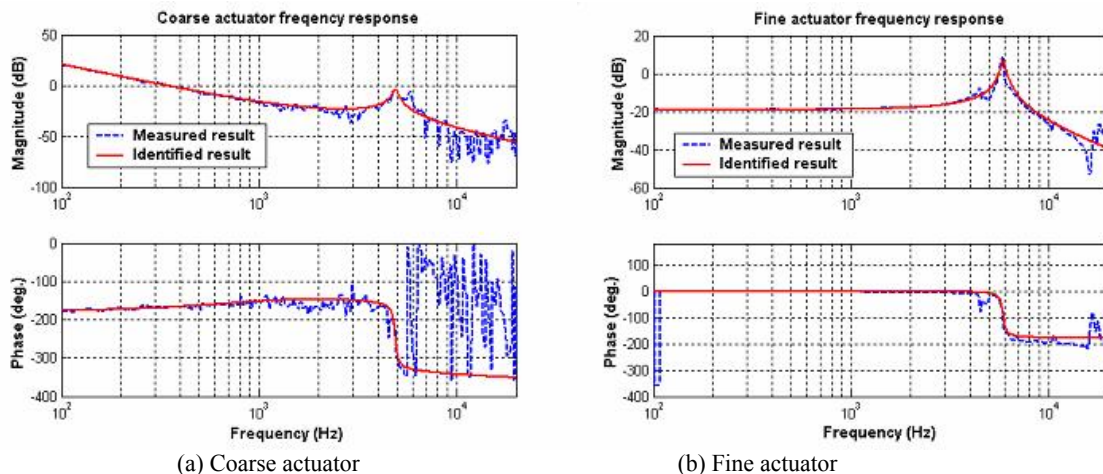


Figure 4: Frequency response of coarse and fine actuators

### 3. Dual servo control

#### 3.1. Track following control

The objective of track following controller is to maintain the head as close as possible to the destination track center under periodic disturbance caused by eccentricity of disk. Thus, track following controller design can be regarded as a disturbance rejection problem. High open loop gain of control system is more desirable to attenuate disturbance.

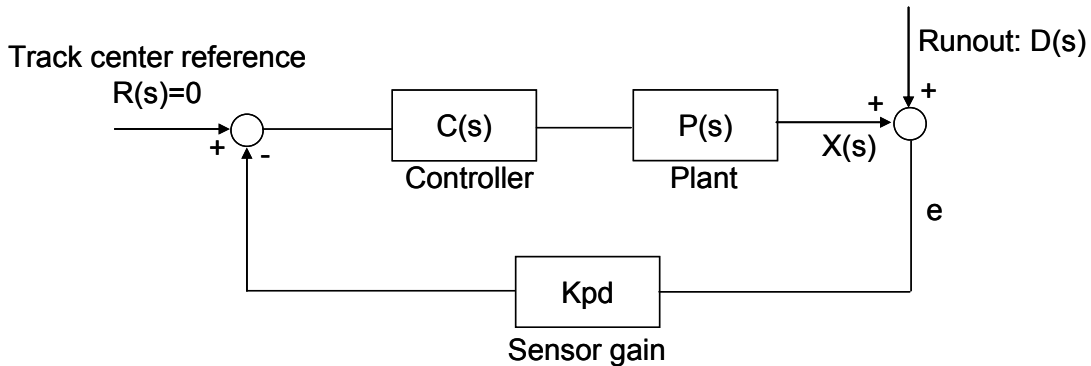


Figure 5: Block diagram of track following control system

The block diagram of track following control system is shown in figure 5. From above block diagram, we can obtain the following equation.

$$e = \frac{C(s)P(s)}{1 + K_{pd}C(s)P(s)}R(s) + \frac{1}{1 + K_{pd}C(s)P(s)}D(s) \quad (3)$$

Track following goal is to maintain the head on the center of destination track. Thus,  $R(s) = 0$  and the error is inversely proportional to the open loop gain. High loop gain is required to attenuate disturbance  $D(s)$  effectively. However, increasing loop gain and bandwidth are restricted by the mechanical resonance of actuator. Moreover, plant uncertainty threatens the system stability and measurement noise deteriorates tracking performance. In the conventional optical pick-up actuator, tracking performance is almost entirely dependent on fine actuator performance. In the manufactured rotary type dual servo actuator, fine actuator provides only  $\pm 500\text{nm}$  moving range. Therefore, both coarse actuator and fine actuator should be properly used for track following. Coarse actuator plays a role to attenuate disturbance with high gain and fine actuator make the bandwidth high.

#### 3.2. PQ method

For assigning proper role to each actuator, the PQ method is used. This reduces the dual-input/single-output (DISO) system control design problem to a single-input/single-output (SISO) design problem.[7] The PQ method is based on parallel type servo structure as shown in figure 6.  $G_1$  is the transfer function of fine actuator,  $G_2$  is the transfer function of coarse actuator,  $C_1$  is the controller of fine actuator,  $C_2$  is the controller of coarse actuator, and  $C_0$  is the total controller.

The first part of PQ method addresses the relative output allocation as a function of frequency and the second part addresses the overall performance of the system. In the first part,  $P$  is defined as the ratio of controller and  $Q$  is defined as the ratio of actuator as shown in figure 7. The product  $PQ$  implies the relative output from the fine actuator output. Thus,  $PQ$  should have large magnitude at low frequency and small magnitude at high frequency. When the magnitude of  $PQ$  is nearly one (0 dB), the output from  $G_1$  and  $G_2$  have nearly the same magnitude. We call this frequency ( $PQ=0$  dB) the hand-off frequency. The phase margin of the  $PQ$  feedback system determines how much the outputs of the two actuators constructively and destructively interfere at the hand-off frequency. At this frequency, the phase margin

should be greater than  $60^\circ$  in order to assure the constructive interference between two outputs. Selecting hand-off frequency is important in PQ method since it determines the moving range of fine actuator while track following.

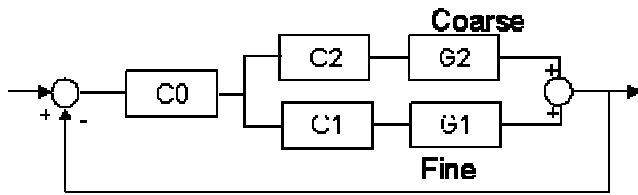


Figure 6: Parallel type structure block diagram

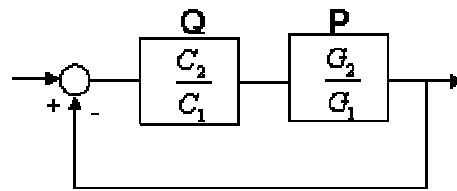


Figure 7: Block diagram of the PQ feedback system

#### 4. Experiments

##### 4.1. Comparison between one servo and dual servo

Figure 8 shows the experiment setup for dual servo track following. Laser doppler vibrometer (OFV3001) is used as a sensor and a commercial DSP controller, dSPACE (DS4003), is used as a controller.

To evaluate disturbance rejection performance, an artificial disturbance is added to sensor output. Figure 9 (a) and (b) show one and dual servo experiment results when the artificial disturbance ( $0.1\mu\text{m}$ -56Hz sinusoidal +  $0.02\mu\text{m}$ -700Hz sinusoidal) is inserted. From figure 9 (a), one servo follows low frequency signal well but it don't follow high frequency signal. However, dual servo follows both of them very well as shown in figure 9 (b). The tracking error change is presented in figure 10. The tracking error is reduced from  $\pm 90\text{nm}$  to  $\pm 25\text{nm}$ . At this time, servo bandwidth is set as 1.5 kHz and the hand-off frequency is 400 Hz.

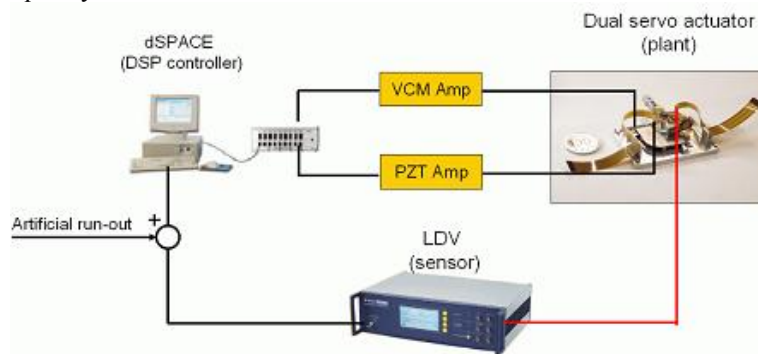
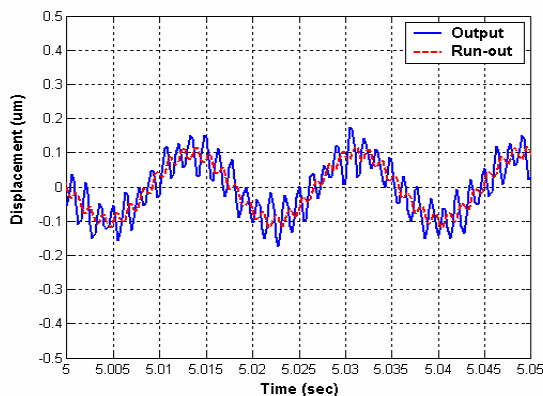
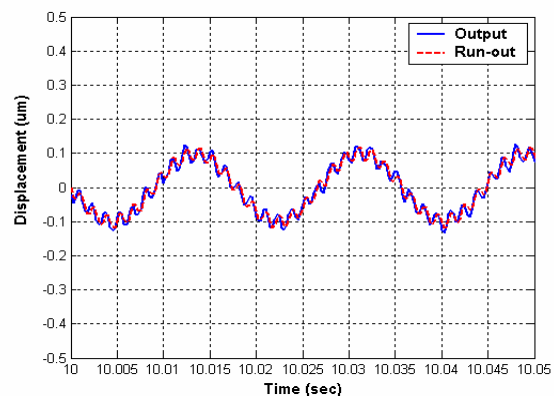


Figure 8: Experiment setup for track following



(a) One servo



(b) Dual servo

Figure 9: One and dual servo track following results

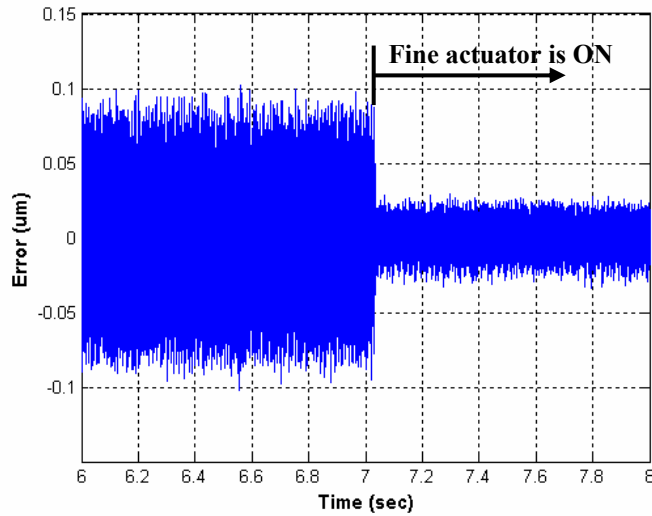
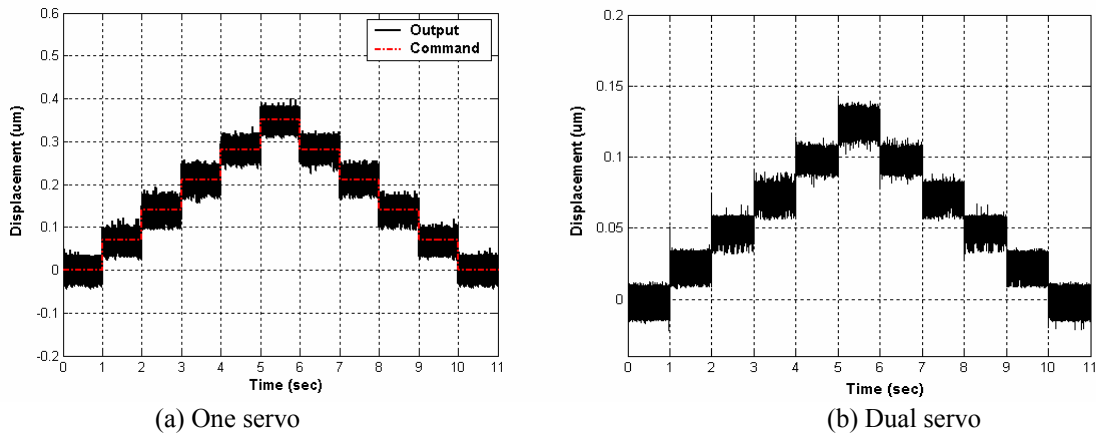


Figure 10: Tracking error reduction when fine actuator is on

To verify the fine actuator another effect, the resolution of one servo system and dual servo system are measured as shown in figure 11 (a) and (b). The resolution of one servo system (only coarse actuator) is 70nm and that of dual servo system (coarse actuator + fine actuator) becomes 25nm. The reason is that fine actuator's flat gain is used in dual servo system above the hand-off frequency. Therefore, disturbance rejection ability of dual servo is better than that of one servo. The sensitivity function comparison between one servo and dual servo systems proves dual servo's better performance in disturbance rejection in figure 12.



(a) One servo

(b) Dual servo

Figure 11: Resolution of one and dual servo

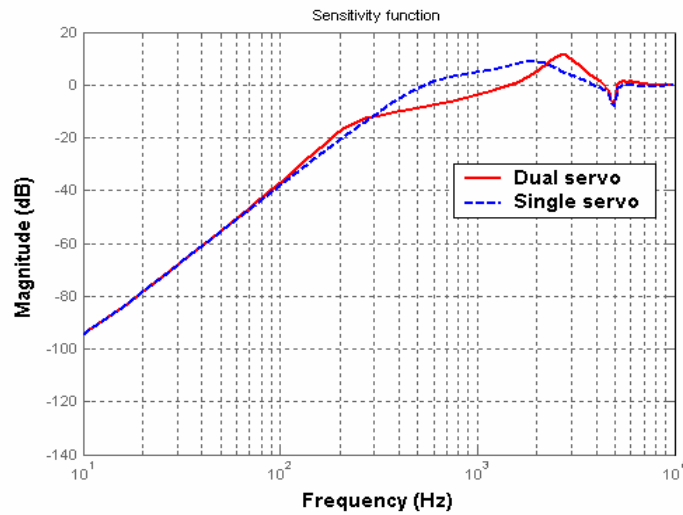


Figure 12: Sensitivity function comparison

#### 4.2. Track following performance

To evaluate the maximum performance of dual servo system, a disturbance (56Hz-1 $\mu$ m sinusoidal) is inserted and the rejection ratio is measured. Figure 13 represents the bode plots according to the variation of total bandwidth of dual servo system. As the total bandwidth becomes large, open loop gain is higher but phase margin is smaller.

The error, measured when the disturbance is 56Hz-1 $\mu$ m sinusoidal, is inserted and the FFT result of the error is shown in figure 14. The maximum disturbance rejection ratio is -63.48dB at 2.5 kHz bandwidth. From this result, we can find that the manufactured dual servo actuator covers  $\pm 44.8\mu$ m disk run-out disturbance at 3360rpm. The maximum radial acceleration of the dual servo actuator is 5.54m/s<sup>2</sup>. Disk run-out rejection ratios according to the variation of total bandwidth of dual servo are summarized in table 1.

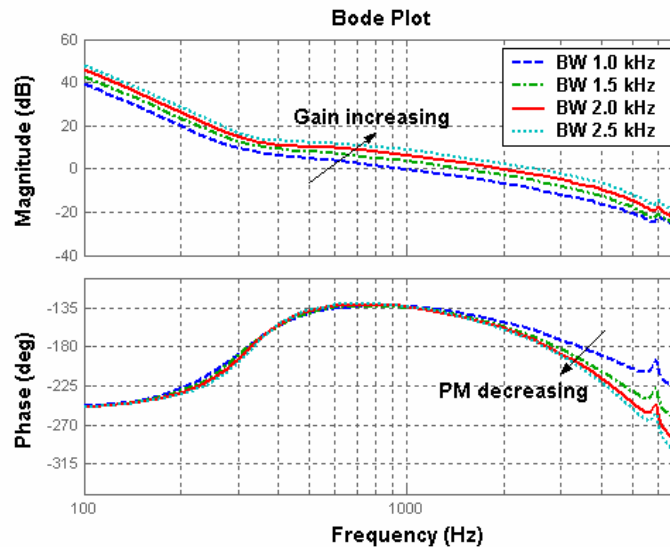


Figure 13: Open loop bode plots of dual servo

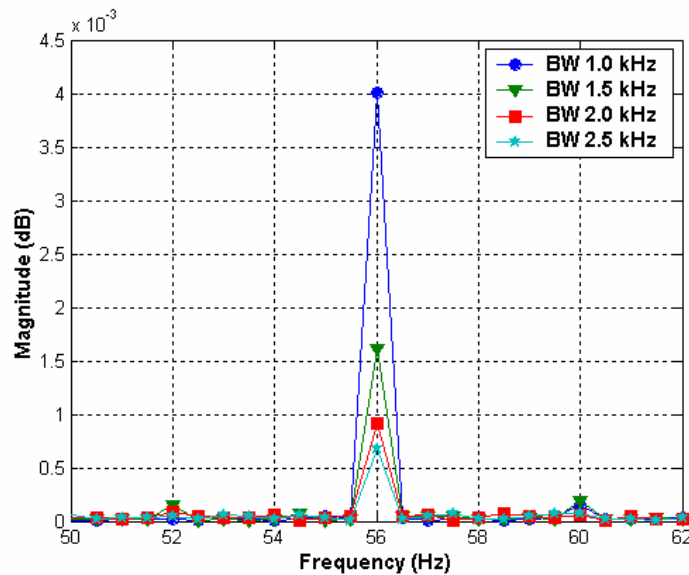


Figure 14: FFT result of error

Bandwidth	1.0 kHz	1.5 kHz	2.0 kHz	2.5 kHz
Input magnitude (56Hz)	1 $\mu\text{m}$	1 $\mu\text{m}$	1 $\mu\text{m}$	1 $\mu\text{m}$
Output magnitude (56Hz)	4.0e-3 $\mu\text{m}$	1.6e-3 $\mu\text{m}$	0.9e-3 $\mu\text{m}$	0.67e-3 $\mu\text{m}$
Rejection ratio	-47.96 dB	-55.92 dB	-60.92 dB	-63.48 dB

Table 1: Disturbance rejection ratio

## 5. Conclusion

The main features of the future optical disk drive such as NFR will be high density, small form factor, and high speed. To satisfy these features, the accuracy of actuator should be increased to read and write the high density data on the disk. In this paper, dual servo actuator for application to NFR is designed and its track following performance is evaluated. Dual servo actuator consists of coarse actuator using MSMA and fine actuator using PMN-PT. From track following performance evaluation, the designed dual servo actuator covers  $\pm 44.8 \mu\text{m}$  disk run-out disturbance at 3360rpm. The resolution of coarse actuator is 70nm and that of dual servo actuator is 25nm. The proposed dual servo actuator shows satisfactory performances to be applied to NFR and it can be applied to other future disk drives.

## References

1. Koichiro K. et al, Jpn. J. Appl. Phys., 41, 3B, 1984, 2002.
2. Sinoda M. et al, Jpn. J. Appl. Phys., 42, 2B, 1101, 2003.
3. Sookyung Kim et al, Proc. of ISOM/ODS, 204, 2002.
4. Kojima, N. et al, Proc. of ODS 2001, 268, 2001.
5. Jaehwa Jeong et al, Jpn. J. Appl. Phys., 43, 4A, 1398, 2004.
6. R.B. Evans et al, IEEE Trans. on Mag., 35, 2, 1999.
7. S. J. Sschroek and W. C. Messner, Proc. of American Control Conference, 6, 4122, 1999.